IV. Conclusion

In this work, a design methodology was introduced to systematically design wideband, electrically small antennas, based on the theory of characteristic modes. This scheme can be used to implement an ideal desired antenna current distribution over a wide frequency range using a finite number of loads at a finite number of ports. The reactive loads at these ports are determined such that this current distribution resonates over a wide frequency band. As an example, the method was applied to a simple wire dipole antenna which was loaded with a set of reactive elements. For this antenna, it was found that non-Foster reactive elements were required to synthesize the reactances determined by (3). Furthermore, it has been demonstrated that through the loading of a dipole antenna using non-Foster elements, the overall antenna bandwidth may be vastly improved. Both pattern and input impedance for the loaded dipole antenna were stabilized over a substantially wider frequency range compared to the unloaded dipole antenna, even without a matching network at the feed point. As expected, improved input impedance bandwidth was obtained when a passive matching network was introduced at the feed port.

References

[1] L. Chu, "Physical limitations of omni-directional antennas," *J. Appl. Phys.*, vol. 19, pp. 1163–1175, 1948.

[2] P. E. Mayes, "Frequency-independent antennas and broad-band derivatives thereof," *IEEE Proc.*, vol. 80, pp. 103–112, Jan. 1992.

[3] S. Licul, J. A. N. Noronha, W. A. Davis, D. G. Sweeney, C. R. Anderson, and T. M. Bielawa, "A parametric study of time-domain characteristics of possible UWB antenna architectures," in *Proc. IEEE 58th Veh. Technol. Conf. VTC 2003-Fall*, 2003, vol. 5, pp. 3110–3114.

[4] J. Quirin, "A Study of high-frequency solid-state negative-impedance converters for impedance loading of dipole antennas," Master's thesis, Univ. Illinois, Chicago, 1970.

[5] A. Poggio and P. Mayes, "Bandwidth extension for dipole antennas by conjugate reactance loading," *IEEE Trans. Antennas Propag.*, pp. 544–547, Jul. 1971.

[6] R. C. Hansen, "Dipole arrays with non-foster circuits," in *Proc. IEEE Int. Symp. on Phased Array Syst. and Technol.*, 2003, pp. 40–44.

[7] E. Antonino-Daviu, M. Cabedo-Fabrés, M. Ferrando-Bataller, and A. Valero-Nogueira, "Wideband double-fed planar monopole antennas," *Electron. Lett.*, vol. 39, pp. 1635–1636, 2003.

[8] M. Cabedo-Fabrés, A. Valero-Nogueira, E. Antonino-Daviu, and M. Ferrando-Bataller, "Modal analysis of a radiating slotted PCB for mobile handsets," in *Proc. Eur. Conf. on Antennas and Propag. EuCAP*, Oct. 2006, vol. 626.

[9] R. Harrington and J. Mautz, "Modal analysis of loaded n-port scatterers," *IEEE Trans. Antennas Propag.*, vol. AP-21, pp. 188–199, Mar. 1973.

[10] S. Sussman-Fort, "Gyrator-based biquad filters and negative impedance converters for microwaves," *Int. J. Microw. Millimeter-Wave CAE*, vol. 8, no. 2, pp. 86–101, 1998.

[11] R. L.-R. James and T. Aberle, *Active Antennas With Non-Foster Matching Networks*, C. A. Balanis, Ed. San Rafael, CA: Morgan and Claypool, 2007, pt. Synthesis Lectures on Antennas.

[12] H. Kim, "Design of negative impedance converters for VHF and UHF applications," Master's thesis, Arizona State Univ., Tempe, 2006.

[13] E. Newman, "The Electromagnetic Surface Patch Code: Version 5," The Ohio State University [Online]. Available: http://esl.eng.ohio-state.edu

[14] K. Obeidat, B. D. Raines, and R. G. Rojas, "Antenna design and analysis using characteristic modes," in *Antennas and Propagation Society Int. Symp.*, 2007, pp. 5993–5996.

[15] A. D. Yaghjian and S. R. Best, "Impedance, bandwidth and Q of antennas," in *Proc. IEEE Antennas Propag. Int. Symp.*, Jun. 2003, pp. 501–504.

[16] H. Carlin and P. Civalleri, *Wideband Circuit Design*. Boca Raton, FL: CRC, 1997.

77 GHz Stepped Lens With Sectorial Radiation Pattern as Primary Feed of a Lens Based CATR

M. Multari, J. Lanteri, J. L. Le Sonn, L. Brochier, Ch Pichot, C. Migliaccio, J. L. Desvilles, and P. Feil

***Abstract*—We describe the design, fabrication and measurements of an axisymmetric dielectric lens, featuring a sectorial radiation pattern at 77 GHz. It will be used as the primary feed of a lens-based compact antenna test range (CATR). Due to symmetry of revolution, the sectorial lens profile can be designed in one dimension by using phase only control. The phase variation is echoed on the lens depth. The resulting stepped lens is simulated using France Telecom Orange Labs SRSRD software ("in-house" software developed for dielectric axisymmetric radiating structures) and measured in an anechoic chamber at 77 GHz. Two lenses were fabricated with different materials: PVC and polyurethane, respectively. Good agreements were obtained between simulations and measurements. Less than 0.2 dB ripple in the central beam are obtained for the polyurethane lens although relatively high secondary lobes occur at 11°. Comparisons between the near field of a CATR illuminated by a small horn providing a uniform amplitude taper and the sectorial lens are conducted using numerical simulations. Results show that on-axis oscillations are reduced from 6 to 1 dB with the sectorial lens.**

***Index Terms*—Compact antenna test range (CATR), dielectric lens, phase control, primary feed, sectorial radiation pattern.**

I. Introduction

This communication describes an axisymmetric dielectric lens, featuring a sectorial radiation pattern at 77 GHz. The sectorial lens is aimed to be used as primary feed for a lens-based compact antenna test range (CATR). Sectorial radiation pattern antennas are widely used in wireless communications, e.g., for base-stations or WIFI terminals [1] but they have also demonstrated their capabilities for measurement system applications such as lens-based CATR [2].

The motivation for using a lens-based CATR is to measure electrically large antennas in the millimeter-wave frequency range. In the last decade, millimeter-wave radar applications have been of increasing interest [3], [4]. Radar antennas have to fulfill the requirements for highly directive antennas such as high gain and low side lobes and result in antenna sizes of several tens of wavelengths. Most of anechoic chambers are too small for obtaining far-field conditions with respect to these antennas sizes. Therefore, a compact range system offers a solution to this test problem. Classical solutions are based on single or more often on double reflectors CATR [5], [6]. But these performing solutions have some important drawbacks such as their low flexibility (they are not easily dismounted when the anechoic chamber has to be used

Manuscript received October 24, 2008; revised June 26, 2009. First published November 06, 2009; current version published January 04, 2010

M. Multari and J. Lanteri are with the Laboratory of Electronics, Antennas and Telecommunications (LEAT), University of Nice-Sophia Antipolis, CNRS, Valbonne 06560, France.

J. L. Le Sonn, L. Brochier, C. Pichot, and C. Migliaccio are with the Laboratory of Electronics, Antennas and Telecommunications (LEAT), University of Nice-Sophia Antipolis, CNRS, Valbonne 06560, France and also with CREMANT, University of Nice-Sophia Antipolis, CNRS, Valbonne 06560, France, and also with France Telecom Orange Labs, Cedex 15 Paris, 75505 (e-mail: claire.migliaccio@unice.fr).

J. L. Desvilles is with Orange Labs, Fort de la Tête de Chien, 06320 La Turbie, France.

P. Feil is with the Department of Microwave Techniques, University of Ulm, Ulm D-89069, Germany (e-mail: peter.feil@uni.ulm.de).

Color versions of one or more of the figures in this communication are available online at http://ieeexplore.ieee.org.

Digital Object Identifier 10.1109/TAP.2009.2036130

0018-926X/$26.00 © 2009 IEEE

Authorized licensed use limited to: KIZ Abt Literaturverwaltung. Downloaded on January 21, 2010 at 10:28 from IEEE Xplore. Restrictions apply.

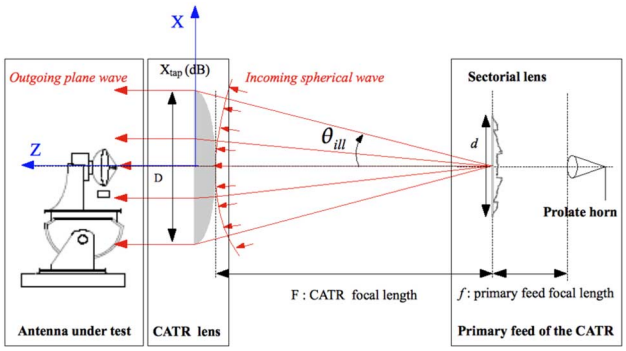

Fig. 1. Lens-based CATR setup.

without CATR arrangement) and high-accuracy fabrication required at mm-waves, and to some extend, the large space they are requiring, especially for double reflector arrangements [7]. An alternative solution could be the use of Holograms [8]–[10] that have proven to be relevant especially at mm and sub-millimeter waves. We have chosen an other alternative solution consisting in lens-based CATR [11] with an outgoing plane wave of 25 cm diameter for W-band measurements. Nevertheless, one has to get rid of the on-axis oscillations (Fresnel spots) due to the strong aperture scattering effects [12] that are reinforced in a lens, due to the internal reflections. A widespread solution is the use of serrations but they may not be sufficient to completely remove the Fresnel spots in the case of the lens-based CATR. For this purpose, we propose a primary feed with a sectorial beam. It has been designed to have uniform amplitude and phase on 68% of the CATR outgoing lens surface. Moreover, the taper illumination rapidly drops at the lens periphery edge. This primary feed is also a small axisymmetrical dielectric lens.

Section II describes the sectorial lens design, simulations and measurements. Due to axisymmetry, the lens profile can be obtained using one-dimensional optimization. It has been carried out using phase only control. The phase variation is echoed on the lens depth. Simulations are performed using the France Telecom Orange labs "in-house" software, so-called SRSRD developed for dielectric axisymmetric radiating structures and based on one-dimensional integral equations [13] for open or closed structures. Former studies have proven this software to be suitable for mm-wave lens simulations [14].

Section III deals with the complete CATR simulations. Comparisons between the near field of a CATR illuminated by a small horn providing a uniform amplitude taper and the sectorial lens are conducted using SRSRD with a 500 mm CATR lens diameter. Finally the CATR performances are discussed.

II. Sectorial Lens Design and MeAsurements

The phase only synthesis has proved to be an efficient method for designing arrays with pre-defined radiation patterns. We apply it to the lens using a quasi-optical approach. The advantage of such a technique is its simplicity of implementation and quick execution although it might be less accurate, compared to more sophisticated methods [15].

A. Sectorial Lens Synthesis and Numerical Simulations

The basic sectorial antenna set-up is shown in Fig. 1 in the *Primary feed of the CATR* box. It consists of a primary feed (prolate horn) illuminating a dielectric lens with focal length f and diameter d. The latter is used for sectorial beam shaping.

The sectorial lens design procedure is based on the quasi-optical approach described in [16]. According to the axi-symmetry of the lens, it has been simplified to the one-dimensional case (1D). The design parameters are the incident and transmitted angles, respectively $\theta_{\rm inc}$ and θ_t, and the electrical length Φ on the lens surface as described in [16]. $\theta_{\rm inc}$ and θ_t are both oriented anti-clockwise. The primary feed radiation pattern is modeled in a first step by $\cos^n \theta_{\rm in}$ function. The main steps of the synthesis method can be summarized as follows.

- The transmitted angle θ_t is classically obtained from the energy conservation as a function of $\theta_{\rm inc}$;
- The electrical length Φ is derived from (1) as described in [16] with the 1D simplification;
- The numerical integration of (1) gives the electrical length that has to be on the lens for the desired pattern;
- Assuming that the phase profile is obtained by changing the lens depth, d_e, we can obtain directly the depth d_e from Φ

$$\frac{d\Phi}{dx} = \sin\theta_t + \sin\theta_{\rm inc}. \tag{1}$$

The phase reference in (1) is taken in the lens centre which leads to $d_e = 0$ at this point. In order to simplify the lens fabrication, it is more convenient to avoid this configuration. Therefore, the phase reference is moved in order to have a null depth at the lens edge. Considering the respective paths of the ray going to the lens edge [left term of (1)] and another one going through the lens [right term of (1)], a new equation leading to the value of d_e is obtained

$$\sqrt{f^2 + (d/2)^2} = \sqrt{(f - d_e)^2 + x^2} + d_e\sqrt{\varepsilon_r} \tag{2}$$

where $y \in [0; d/2]$.

Finally, d_e is obtained from solving (2).

Before going into design considerations, let us note that the quasi-optical approach leads to a stepped lens. As a consequence, a large lens will provide a large number of steps and make the lens fabrication more complex. Therefore this method is suitable for electrically small lenses.

The synthesis method described above is implemented with Scilab software [17]. The desired sectorial pattern $G(\theta_t)$ is chosen to be uniform over $\pm\theta_0$ and to drop rapidly beyond according to (3)

$$G(\theta_t) = 1 - \left|\frac{\tan\theta_t}{\tan\theta_0}\right|^{15}. \tag{3}$$

According to the desired configuration of the compact range, θ_0 is chosen to be 5°. The design frequency is 77 GHz. The primary feed of the sectorial lens is designed to perform a prolate radiation pattern for low secondary lobes purposes [18]. The prolate horn dimensions and measurements are shown in Fig. 2(a) and (b) respectively. It is designed for an illumination at -20 dB on the edges of the lens and corresponds to a focal length to diameter ratio of 1.

Applying the method described above, a sectorial lens with diameter (d) of 50 mm, [about 13 λ. and using 20 x-samples per wavelength for solving (2)] was designed. The total number of steps is 270. The stepped lens profile given in the Annex is obtained for polyurethane $(\varepsilon_{\rm r} = 4)$. The large steps correspond to phase angle close to 180°. The design led to changes in the sign of the amplitude (which is equivalent to a 180° phase shift) due to the phase reference taken from (2). In counterpart, they create shadowing areas.

Fabrication errors and focal length displacements have to be studied since we are working at millimeter waves. These errors can be close to the step dimensions of the fabricated lens. Therefore simulations are conducted with SRSRD using ± 50 μm errors randomly distributed on the lens profile. The same way, ± 1 mm focal length displacements are

Authorized licensed use limited to: KIZ Abt Literaturverwaltung. Downloaded on January 21, 2010 at 10:28 from IEEE Xplore. Restrictions apply.

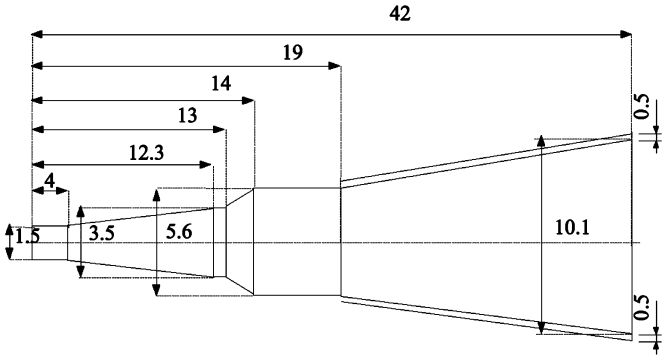

(a)

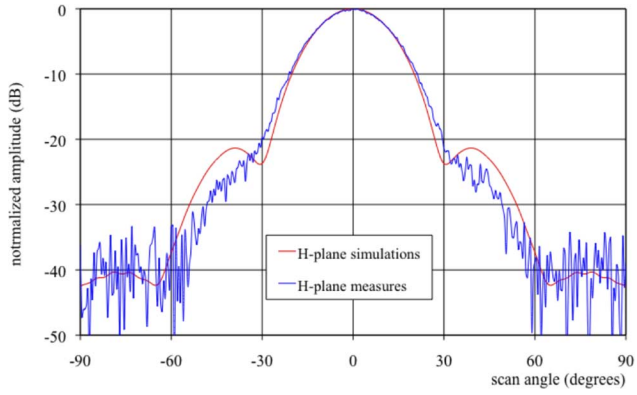

(b)

Fig. 2. (a) Primary feed: prolate horn—dimensions in mm. (b) Primary feed measurements at 77 GHz.

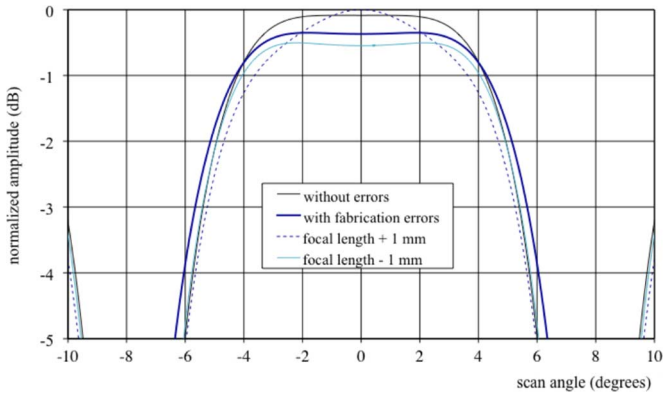

Fig. 3. Fabrication and focal length errors.

investigated. Results are plotted in Fig. 3, the total oscillation does not exceed 1 dB.

B. Sectorial Lens Measurements and Discussion

A first lens has been fabricated using PVC. Despite a relative good agreement with simulations, a critical, for CATR application, 1 dB oscillation in the E-plane is obtained. Looking at the lens fabrication, one can guess that debris remain in the lens grooves. They are probably due to the standard milling technique used for machining PVC. In order to overcome this difficulty, a second lens was fabricated using polyurethane. The complete sectorial lens set-up is shown in Fig. 4.

Fig. 5 shows the comparisons between measurements and simulations. The focal length has been fitted at 51 mm in order to suppress the ripples in the main lobe. Measurements are in very good agreement with simulations within the sectorial behavior of the radiation pattern. The remaining oscillation has been drastically reduced to 0.2

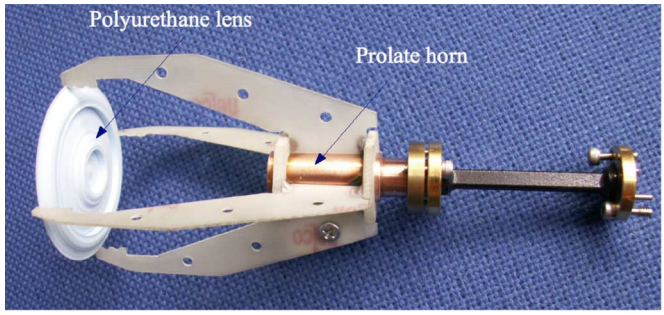

Fig. 4. Sectorial lens picture.

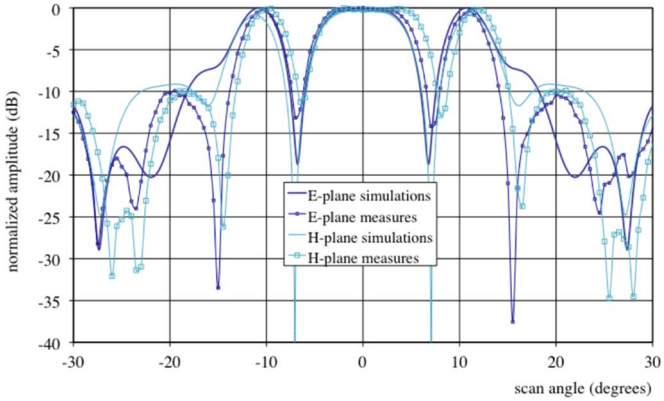

Fig. 5. Simulated and measured radiation pattern at 77 GHz.

dB. Frequency measurements were also conducted showing good radiation pattern stability over the frequency range from 75 to 79 GHz. The sectorial pattern is achieved within $\pm 5^{\circ}$. High secondary lobes occur at $\pm 11^{\circ}$ given that the design template was given only up to the desired zeros of the diagram.

In a large anechoic chamber implementation, they are not critical for our application because they will be the spillover part of the illumination of the CATR and hence will be very low compared to the focusing done by the lens of the CATR. This effect is reinforced with increasing the size of the lens CATR. Nevertheless the high lobes levels at 11° may affect the quality of the quiet zone, given that the CATR is to be built in a small anechoic chamber, especially because of the possible reflections on the walls. Hence, some absorbing material will be used around the lens. This solution has been successfully tested in a previous study with a uniform illumination on the CATR-lens [19].

III. Application to the CATR

If we aim to design a CATR, one has to face the trade-off between the strong edge diffraction, that occur with uniform illumination and the decrease of the quiet zone spot caused by the reduction of the illumination taper. The sectorial illumination seems to be the ideal compromise since it provides a uniform illumination while having a rapid drop at the CATR edges.

A previous experimental study, conducted in 2006 [19] on a 500 mm diameter PVC-lens based CATR, has shown that high on-axis oscillations occur in the near field distribution when a uniform illumination is applied to the CATR. This effect has been also previously demonstrated from theoretical studies in circular apertures [20]. In order to check this behavior, our lens-CATR configuration was simulated using a uniform illumination taper. For this purpose, the primary feed is a small standard circular horn providing 1 dB taper at the CATR-lens edges. The CATR-lens has a hyperbolic profile and is made of PVC. Simulations were conducted at 77 GHz.

Authorized licensed use limited to: KIZ Abt Literaturverwaltung. Downloaded on January 21, 2010 at 10:28 from IEEE Xplore. Restrictions apply.

TABLE I

ANNEX: SECTORIAL HALF-LENS DIMENSIONS FOR $\varepsilon_r = 4$, x = lens radius, z = lens depth

x (mm)	z (mm)	x (mm)	z (mm)	x (mm)	z (mm)	x (mm)	z (mm)	x (mm)	z (mm)
0.00	2.73	4.87	2.05	9.94	2.84	15.00	1.80	20.06	2.34
0.19	2.68	5.06	2.05	10.13	2.73	15.19	1.73	20.26	2.29
0.39	2.61	5.26	2.05	10.32	2.69	15.39	1.63	20.45	2.23
0.58	2.57	5.45	2.04	10.52	2.69	15.58	1.53	20.65	2.17
0.78	2.55	5.65	2.05	10.71	2.71	15.78	1.41	20.84	2.11
0.97	2.51	5.84	4.36	10.91	2.70	15.97	1.29	21.04	2.03
1.17	2.44	6.04	4.38	11.10	2.67	16.17	1.18	21.23	1.94
1.36	2.36	6.23	4.40	11.30	2.61	16.36	1.09	21.43	1.82
1.56	2.29	6.43	4.41	11.49	2.55	16.56	1.01	21.62	1.68
1.75	2.25	6.62	4.41	11.69	2.48	16.75	0.95	21.82	1.51
1.95	2.21	6.82	4.39	11.88	2.42	16.95	0.88	22.01	1.33
2.14	2.18	7.01	4.36	12.08	2.37	17.14	0.81	22.21	1.15
2.34	2.17	7.21	4.31	12.27	2.34	17.34	0.71	22.40	0.98
2.53	2.16	7.40	4.26	12.47	2.31	17.53	0.61	22.60	0.83
2.73	2.17	7.60	4.19	12.66	2.28	17.73	0.49	22.79	0.69
2.92	2.20	7.79	4.10	12.86	2.25	17.92	2.56	22.99	0.57
3.12	2.24	7.99	3.98	13.05	2.22	18.12	2.47	23.18	0.47
3.31	2.29	8.18	3.85	13.25	2.18	18.31	2.41	23.38	0.38
3.51	2.33	8.38	3.76	13.44	2.15	18.51	2.37	23.57	0.30
3.70	2.34	8.57	3.75	13.64	2.12	18.70	2.36	23.77	0.22
3.90	2.33	8.77	3.75	13.83	2.09	18.90	2.37	23.96	0.16
4.09	2.26	8.96	3.70	14.03	2.06	19.09	2.39	24.16	0.12
4.29	2.16	9.16	3.55	14.22	2.01	19.29	2.41	24.35	0.08
4.48	2.07	9.35	3.35	14.42	1.96	19.48	2.42	24.55	0.06
4.68	2.04	9.55	3.17	14.61	1.91	19.68	2.41	24.74	0.04
		9.74	3.00	14.81	1.86	19.87	2.38	24.94	0.03

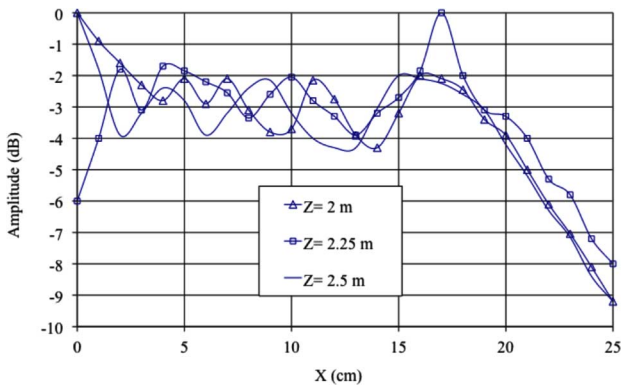

Fig. 6. CATR near field, D = 500 mm, F = 2 m, $\theta_{ill} = 7°$, $X_{tap} = 10$ dB for the uniform feed, $X_{tap} = 1$ dB for the sectorial illumination.

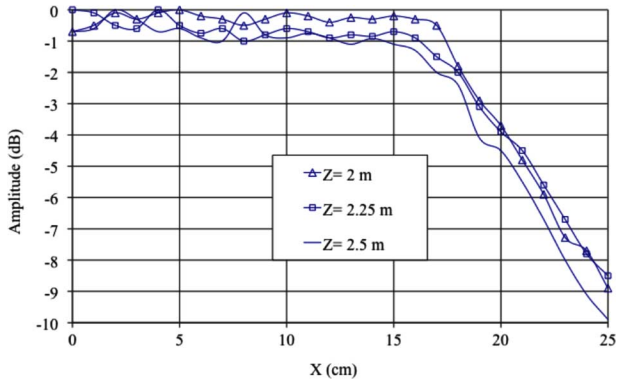

Fig. 7. Same CATR configuration as in Fig. 6 with an sectorial illumination.

The amplitude field distributions at different down range distances (Z) from the CATR-lens are shown in Fig. 6. The coordinate system (X, Z) is defined according to Fig. 1, where X denotes the displacement along the lens radius and Z the distance from the center of the flat border lens to the AUT. The on-axis (X = 0) oscillations between Z = 2 and Z = 2.5 m are 6 dB. In addition, the ripple in the quite zone (along X) is 4 dB. The same simulation has been conducted using the polyurethane sectorial lens and the results are shown in Fig. 7. It is obvious that the sectorial lens dramatically reduces the ripple in the quite zone.

The maximum quiet zone radius is obtained at Z = 2 m and is of 170 mm that corresponds to 68% of the CATR-lens surface. Within this zone, the maximum amplitude oscillation is 1 dB and the phase ripple does not exceed 8°. Moreover, the quiet zone depth (along Z-axis) is 0.5 m.

The installation of the CATR antenna system requires a space of 4.1 m (along Z). Furthermore, the rotation of the AUT also needs some space that has been estimated to 50 cm and some margin for the CATR construction has to be taken. Therefore, the total size of the CATR should not exceed 5 m. This overall configuration is interesting as we can build a compact test range within a small anechoic chamber.

IV. CONCLUSION

This communication describes the design, simulation and measurement of a new sectorial lens for primary feed of a lens-based mm-wave

Authorized licensed use limited to: KIZ Abt Literaturverwaltung. Downloaded on January 21, 2010 at 10:28 from IEEE Xplore. Restrictions apply.

CATR. The design procedure, based on the one-dimensional quasi-optical approach, despite of its simplicity and approximations that are made regarding the internal lens reflections, is quite efficient for computing the sectorial lens profile. The axisymmetry of the lens makes it easy, in principle, to fabricate. Nevertheless the choice of the dielectric material is important since it has to be compatible with the milling technique for ensuring a good surface quality of finish. Therefore, polyurethane material is preferred to PVC. Very good agreement has been obtained between measurements and simulations carried out with SRSRD. This is a key point because the lens design procedure neglects some important lens features such as the internal reflections or step shadowing. From this knowledge, we can perform quite accurate simulations using SRSRD. The above-mentioned effects were quantified and their influences on the final CATR setup were studied.

REFERENCES

[1] S. Qi and K. Wu, "Leakage and resonance characteristics of radiating cylindrical dielectric structure suitable for use as a feeder for high-efficient omnidirectional/sectorial antenna," *IEEE Trans. Antennas Propag.*, vol. 46, no. 11, pp. 1767–1773, Sep. 1998.

[2] T. Hirvonen, J. Tuovinen, and A. V. Räisänen, "Lens-type compact antenna test range at mm-waves," in *Proc. 21st Eur. Microw. Conf.*, Stuttgart, Germany, Oct. 1991, vol. 2, pp. 1079–1083.

[3] B. D. Nguyen, C. Migliaccio, Ch. Pichot, K. Yalmamoto, and N. Yonemoto, "W-band fresnel zone plate reflector for helicopter collision avoidance radar," *IEEE Trans. Antennas Propag.*, vol. 55, no. 5, pp. 1452–1456, May 2007.

[4] W. Mayer, M. Meilchen, W. Grabherr, P. Nüchter, and R. Gühl, "Eight channel 77 GHz front-end module with high-performance synthesized signal generator for FM-CW sensor applications," *IEEE Microw. Theory Tech.*, vol. 52, no. 3, pp. 993–1000, Mar. 2004.

[5] E. K. Walton and J. D. Young, "The Ohio state university compact range cross-section measurement range," *IEEE Trans. Antennas Propag.*, vol. 32, no. 11, pp. 1218–1233, Nov. 1984.

[6] C. W. I. Pistorius, G. C. Clerici, and W. D. Burnside, "A dual chamber Gregorian subreflector system for compact range applications," *IEEE Trans. Antennas Propag.*, vol. 37, no. 3, pp. 305–313, Mar. 1989.

[7] G. Forma, D. Dubruel, J. Marti-Canales, M. Paquay, G. Crone, J. Tauber, M. Sandri, F. Villa, and I. Ristorcelli, "30-70-100-320 GHz radiation measurements for the radio frequency qualification model of the Planck satellite," presented at the 1st Eur. Conf. on Antennas Propag., (EuCAP2006), Nice, France, Nov. 6–10, 2006, paper 349443.

[8] J. Meltaus, J. Salo, E. Noponen, M. M. Salomaa, V. Viikari, A. Lönnqvist, T. Koskinen, J. Sáily, J. Hakli, J. Ala-Laurinaho, J. Mallat, and A. V. Räisänen, "Millimeter-wave beam shaping using holograms," *IEEE Microw. Theory Tech.*, vol. 51, no. 4, pp. 1274–1279, Apr. 2003.

[9] J. Häkli, T. Koskinen, A. Lönnqvist, J. Säily, V. Viikari, J. Mallat, J. Ala-Laurinaho, J. Tuovinen, and A. V. Räisänen, "Testing of a 1.5-m reflector antenna at 322 GHz in a CATR based on a hologram," *IEEE Trans. Antennas Propag.*, vol. 53, no. 10, pp. 3142–3150, Oct. 2005.

[10] A. Lönnqvist, T. Koskinen, J. Hakli, J. Sáily, J. Ala-Laurinaho, J. Mallat, V. Viikari, J. Tuovinen, and A. V. Räisänen, "Hologram-based compact range for submillimeter-wave antenna testing," *IEEE Trans. Antennas Propag.*, vol. 53, no. 10, pp. 3151–3159, Oct. 2005.

[11] Menzel and B. Huder, "Compact range for millimeter-wave frequencies using a dielectric lens," *Electron. Lett.*, vol. 20, pp. 768–769, Sep. 1984.

[12] G. Bruhat, *Optique*. France: Masson, 1959, 5ème edition, RO30013068.

[13] A. Berthon and R. Bills, "Integral equation analysis for radiating structures of revolution," *IEEE Trans. Antennas Propag.*, vol. 49, no. 4, pp. 159–170, Feb. 1989.

[14] C. Migliaccio, J.-Y. Dauvignac, L. Brochier, J.-L. Le Sonn, and Ch. Pichot, "W-band high gain lens antenna for metrology and radar applications," *Electron. Lett.*, vol. 40, no. 22, pp. 1394–1396, Oct. 28, 2004.

[15] A. P. Pavacic, D. L. Del Rio, J. R. Mosig, and G. V. Eleftheriades, "Three dimensional ray tracing theory to model internal reflections in off-axis lens antennas," *IEEE Trans. Antennas Propag.*, vol. 54, no. 2, pp. 604–612, Feb. 2006.

[16] R. Leberer and W. Menzel, "A dual planar reflectarray with synthesized phase and amplitude distribution," *IEEE Trans. Antennas Propag.*, vol. 53, no. 11, pp. 3534–3539, Nov. 2005.

[17] [Online]. Available: www.scilab.org

[18] J. Lanteri, C. Migliaccio, J.-Y. Dauvignac, and Ch. Pichot, "Reflectarray using a prolate feed at 94 GHz," in *Proc. IEEE AP-S*, San Diego, Jul. 5–11, 2008, pp. 1–4.

[19] M. Multari, C. Migliaccio, J.-Y. Dauvignac, L. Brochier, J.-L. Le Sonn, Ch. Pichot, W. Menzel, and J.-L. Desvilles, "Investigation of low-cost compact range W-band," in *Proc. EuCAP*, Nice, Nov. 6–10, 2006, pp. 1–6.

[20] R. C. Rudduck and C. L. J. Chen, "New plane wave spectrum formulation for the near-field of circular apertures," *IEEE Trans. Antennas Propag.*, vol. 24, no. 4, pp. 438–449, Jul. 1976.

A Single-Layer Ultrawideband Microstrip Antenna

Qi Wu, Ronghong Jin, and Junping Geng

***Abstract*—A single-layer microstrip antenna for ultrawideband (UWB) applications, in which an array of rectangular microstrip patches was arranged in the log-periodic way and proximity-coupled to the microstrip feeding line, is presented. In order to reduce the number of microstrip patches in the UWB log-periodic arrays, a large scale factor $k = 1.1$ was firstly reported and proved to be highly effective. Furthermore, instead of using an absorbing terminal loading, a novel loss-free compensating stub was proposed. Detailed parameters study was also presented for better understanding of the proposed antennas. The impedance bandwidth (measured $VSWR < 2.5$) of an example antenna with only 11 elements is from 2.26–6.85 GHz with a ratio of about 3.03:1. Both numerical and experimental results show that the proposed antenna has stable directional radiation patterns, very low-profile and low fabrication cost, which are suitable for various broadband applications.**

***Index Terms*—Directional antennas, log-periodic antennas, microstrip antennas, ultrawideband (UWB) antennas.**

I. INTRODUCTION

Currently, there are increasing demands for novel ultrawideband (UWB) antennas with low-profile structures and constant directional radiation patterns for both commercial and military applications [1], [2]. Unfortunately, most of the mature UWB antennas like equiangular and Archimedean spirals [3], planar monopoles [4], [5] and wide slot antennas [6], [7] have inherently bi-directional or omnidirectional radiation patterns, which were unsuitable for conformal placement on certain platforms. Cavity-backed log-periodic slot antennas [8] could be integrated compactly into various aircrafts, but they could only provide end-fire radiation patterns and have somewhat high profile.

On the other hand, microstrip antennas have some attractive merits like very low-profile and broadside radiation patterns with medium gains, which have been considered as excellent conformal radiators [9] for a long time. However, a traditional single-element microstrip antenna has inherently narrow impedance bandwidth. In the 1980s, the

Manuscript received January 06, 2009; revised May 10, 2009. First published July 14, 2009; current version published January 04, 2010.

The authors are with the Department of Electronic Engineering, Shanghai Jiao Tong University, Shanghai 200240, China (e-mail: wuqi_2004@sjtu.edu.cn).

Color versions of one or more of the figures in this communication are available online at http://ieeexplore.ieee.org.

Digital Object Identifier 10.1109/TAP.2009.2027728

0018-926X/$26.00 © 2009 IEEE

Authorized licensed use limited to: KIZ Abt Literaturverwaltung. Downloaded on January 21, 2010 at 10:28 from IEEE Xplore. Restrictions apply.